arXiv:1304.2527v1 [quant-ph] 9 Apr 2013

Extreme spin squeezing for photons

Morgan W. Mitchell[1, 2, *] and Federica A. Beduini[1, †]
[1] *ICFO-Institut de Ciencies Fotoniques, Av. Carl Friedrich Gauss, 3, 08860 Castelldefels, Barcelona, Spain.*
[2] *ICREA-Institució Catalana de Recerca i Estudis Avançats, Lluis Companys 23, 08010 Barcelona, Spain*

(Dated: April 10, 2013)

We apply spin-squeezing techniques to identify and quantify highly multi-partite photonic entanglement in polarization-squeezed light. We consider a practical single-mode scenario, and find that Wineland-criterion polarization squeezing implies entanglement of a macroscopic fraction of the total photons. A Glauber-theory computation of the observable N-photon density matrix, with N up to 100, finds that N-partite entanglement is observable despite losses and without post-selection. We estimate that existing detectors could observe ~ 1000-partite entanglement from a few dB of polarization squeezing.

Introduction - Multi-particle entangled states are of central importance in quantum computing and quantum simulation, where entanglement gives an advantage that grows rapidly with the size of the entangled system. Multi-particle entanglement has been demonstrated by controlled interactions of individual particles in a variety of systems, including trapped ions [1], liquid-state NMR [2], solid state devices [3] and photons [4–6]. The current record is 14 particles [7] (ions).

A complementary approach works with large ensembles and uses squeezing, either dynamical or measurement-based, to generate a non-classical state of the ensemble. Sørensen and coworkers [8] showed that for spin-1/2 atoms, spin squeezing implies entanglement within the ensemble. Similar results have been found for higher-spin atoms [9], for multi-partite entanglement [10–12] and for other kinds of squeezing [13]. Squeezing can generate highly multi-partite entanglement, the "extreme spin squeezing" of [10], because it acts simultaneously on a large number of particles. Squeezing of spin ensembles has been reported [14–19], implying pairwise entanglement of macroscopic numbers of particles and at least 80-partite entanglement [14], although microscopic correlations have not been directly observed.

Here we consider the analogous situation for photons. As photons have two possible polarizations, the natural analogy is to squeezing of spin-1/2 ensembles. Unlike atoms, no superselection rule prevents photonic systems from existing in a superposition of different particle numbers. Indeed, these superpositions are the defining feature of optical coherence [20, 21]. Because optical coherence at all orders is abundantly present in laser light [20], it is arguably a classical, not a quantum, resource. Optical coherence is nonetheless very useful for generating photonic entanglement, as we show. We describe a simple scenario that requires as input only one weak squeezed-vacuum state and one coherent state, and which generates N-partite entanglement for arbitrarily large N. We estimate that ~ 1000-partite entanglement should be directly observable with existing detectors.

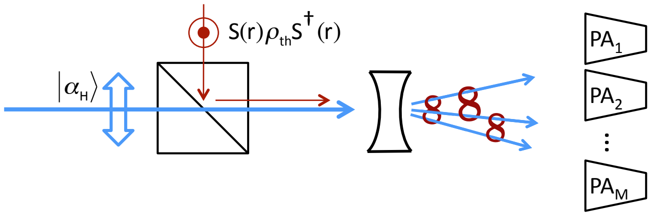

FIG. 1. Scenario for entanglement generation: a horizontally-polarized coherent state $|\alpha_H\rangle$ is combined with a vertically-polarized squeezed state $S(r)\rho_{\rm th}S^\dagger(r)$. The resulting polarization-squeezed state is symmetrically dispersed by a lens to an array of polarization analyzers (PA), each consisting of wave-plates, a polarizing beamsplitter, and single-photon detectors. Under conditions typical of squeezing experiments, nearly all of the photons originate in the coherent beam and become polarization entangled via coherence with the much weaker squeezed beam.

Scenario - We consider a single-mode pulse of polarization-squeezed light [22, 23] described by the state

$$\rho = \rho_H \otimes \rho_V \tag{1}$$

consisting of a coherent state $\rho_H = |\alpha_H\rangle\langle\alpha_H|$ in the horizontal (H) polarization and a squeezed thermal state $\rho_V = \hat{S}(r)\rho_{\rm th}\hat{S}^\dagger(r)$ in the vertical (V). Here $\hat{S}^\dagger(r)a_V\hat{S}(r) = a_V\cosh r - a_V^\dagger\sinh r$ defines the squeeze operator $\hat{S}$ and $\rho_{\rm th} \equiv \sum_n n_{\rm th}^n/(1+n_{\rm th})^{n+1}|n\rangle\langle n|$ is the thermal state. It is convenient to parametrize this state by $n_{\rm c} \equiv |\alpha|^2$, $n_{\rm s} \equiv \sinh^2|r|$ and $n_{\rm th}$. States with this description can be produced by combining squeezed and coherent pulses on a polarizing beam-splitter [24] or by polarization self-rotation [25] of a coherent pulse. Regarding ρ_V, for simplicity we take r real and negative and define $T^2 \equiv 1 + 2n_{\rm th}$, $A \equiv \sqrt{n_{\rm s}} + \sqrt{n_{\rm s}+1}$, so that the quadratures $x \equiv (a_V + a_V^\dagger)/2$, $p \equiv i(a_V^\dagger - a_V)/2$ have variances ${\rm var}(x) = T^2A/4$, ${\rm var}(p) = T^2/(4A^2)$. Note that p is squeezed if $n_{\rm s} > n_{\rm th}^2/(1+2n_{\rm th})$.

Macroscopic quantum features - The quantum description of the macroscopic polarization is given by the Stokes operators [26] $S_0 = (a_H^\dagger a_H + a_V^\dagger a_V)/2$, $S_x = (a_H^\dagger a_H - a_V^\dagger a_V)/2$, $S_z = -i(a_H^\dagger a_V - a_V^\dagger a_H)/2$, $iS_y = [S_z, S_x]$. We find $2\langle S_0\rangle = n_{\rm c} + n_{\rm s} + n_{\rm th} + 2n_{\rm s}n_{\rm th}$, $2\langle S_x\rangle = n_{\rm c} - n_{\rm s} - n_{\rm th} -$

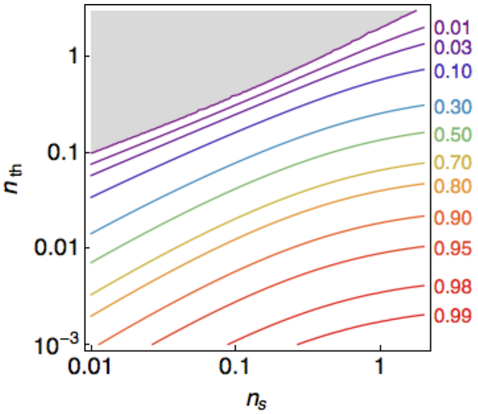

FIG. 2. (color online) Entanglement depth as a fraction of total photon number $k/(2\langle S_0\rangle)$ in the thermodynamic limit $\langle S_0\rangle \to \infty$, shown versus squeezing $n_{\rm c}$ and thermal noise $n_{\rm th}$. Contour values shown on right. Grey region indicates non-entangled regime $k = 1$, which coincides with non-squeezed states.

$2n_{\rm s}n_{\rm th}$. If $\alpha = |\alpha|$ so that S_z is the lower-noise Stokes component, we find $4{\rm var}(S_z) = n_{\rm c}(1+2n_{\rm s}-2\sqrt{n_{\rm s}(n_{\rm s}+1)})(1+2n_{\rm th})$. The state is squeezed by the Wineland criterion [27], ${\rm var}(S_z) < \frac{1}{2}|\langle S_x\rangle|$ if $n_{\rm s} > n_{\rm th}^2/(2n_{\rm th}+1)$, the same condition as for ρ_V quadrature squeezing.

Microscopic quantum features - To find the depth of entanglement k, i.e., the minimum size of entangled clusters in the state, we use the theory of Sørensen and Mølmer [10], extended by Hyllus *et al.* [28] to indefinite numbers of particles. For given degree of polarization $\mathcal{P} \equiv \langle S_x\rangle / \langle S_0\rangle$ and polarization noise $\mathcal{V} \equiv {\rm var}(S_z)/\langle S_0\rangle$, $k/2$ is the minimum spin capable of producing $(\mathcal{P},\mathcal{V})$. As $n_{\rm c} \to \infty$, $\mathcal{V} \to \frac{1}{2}(1+2n_{\rm s}-2\sqrt{n_{\rm s}(n_{\rm s}+1)})(1+2n_{\rm th})$ while $\mathcal{P} \to 1$. If $\mathcal{V} < \frac{1}{2}$, i.e., if the state is squeezed, then $P \to 1$ implies $k \to \infty$, indicating of arbitrarily large groups of entangled particles. As shown in Appendix I, in this limit k is proportional to the total number of photons $2\langle S_0\rangle$. Polarization squeezing evidently implies a *giant connected component* in the language of graph theory [29] and entanglement percolation [30, 31]. The connected component can include nearly all photons for modest $n_{\rm s}$, $n_{\rm th}$, see Figure 2.

Observable entanglement - Reconstruction of density matrices from coincidence rates is the standard method for characterizing multi-photon states [32]. The coincidence rates are described by Glauber photo-detection theory [20], while the reconstruction employs quantum state tomography. The results indicate not the ideal ρ of Eq. (1), but rather an *observable density matrix* (ODM) $\mathcal{R}^{(N)}$ for each possible number of detected photons N. This properly accounts for loss of information to the environment in the form of undetected photons; $\mathcal{R}^{(N)}$ is usually mixed even when ρ is a pure state.

Concretely, we imagine passively splitting the beam to a large number $M \gg N$ of analyzers, as illustrated in Figure 1, and using the observed detections to infer the locations of the photons. The d'th detection mode is described by the annihilation operator $a_{d,p} = \sqrt{M^{-1}}a_p+\sqrt{1-M^{-1}}a_{d,p}^{(\rm aux)}$ where p is the polarization and $a_{d,p}^{(\rm aux)}$ describes an auxiliary mode, required for unitarity of the splitting process and assumed to be in a vacuum state. Because the splitting is polarization-independent, the output retains the exchange symmetry of the initial state ρ, and thus only the polarizations of the detected photons, not their arrival locations, are relevant to the entanglement characterization.

For a single pulse, the probability of coincidence detection with polarizations $\mathbf{p}^{(1)},\ldots,\mathbf{p}^{(N)}$ at detectors $1\ldots N$ is given by

$$\begin{aligned} P_{\{\mathbf{p}\}}^{(N)} &\propto \left\langle a_{1,\mathbf{p}^{(1)}}^\dagger \ldots a_{N,\mathbf{p}^{(N)}}^\dagger a_{N,\mathbf{p}^{(N)}} \ldots a_{1,\mathbf{p}^{(1)}} \right\rangle \\ &\propto \left\langle a_{\mathbf{p}^{(1)}}^\dagger \ldots a_{\mathbf{p}^{(N)}}^\dagger a_{\mathbf{p}^{(N)}} \ldots a_{\mathbf{p}^{(1)}} \right\rangle, \end{aligned} \tag{2}$$

where the second line follows from the definition of $a_{d,p}$ and the fact that the vacuum contributes nothing to the normally-ordered expectation. We employ the computational basis $|\boldsymbol{\pi}_0\rangle \equiv |H,\ldots,H,H\rangle, |\boldsymbol{\pi}_1\rangle \equiv |H,\ldots,H,V\rangle,\ldots,|\boldsymbol{\pi}_{2^N-1}\rangle \equiv |V,\ldots,V,V\rangle$ to describe the (unnormalized) ODM

$$R_{|\boldsymbol{\pi}_i\rangle,\langle\boldsymbol{\pi}_j|}^{(N)} \propto \left\langle a_{\boldsymbol{\pi}_i^{(1)}}^\dagger \ldots a_{\boldsymbol{\pi}_i^{(N)}}^\dagger a_{\boldsymbol{\pi}_j^{(N)}} \ldots a_{\boldsymbol{\pi}_j^{(1)}} \right\rangle, \tag{3}$$

where $\boldsymbol{\pi}_i^{(l)}$ indicates the polarization of the l'th photon in the basis element $|\boldsymbol{\pi}_i\rangle$. We normalize $\mathcal{R}^{(N)} \equiv R^{(N)}/{\rm Tr}[R^{(N)}]$ so that

$$P_{\{\mathbf{p}\}}^{(N)} = {\rm Tr}[\Pi_{\vec{p}}\mathcal{R}^{(N)}] \tag{4}$$

resembles the Born rule. Here $\vec{p}$ is defined to give $\mathbf{p}^{(i)} = \sum_j p_j \boldsymbol{\pi}_j^{(i)}$, so that $\Pi_{\vec{p}} \equiv \vec{p}\wedge\vec{p}$ is a projector onto $\{\mathbf{p}\}$.

Nature of the entanglement - $\mathcal{R}^{(N)}$ is in general a mixture of symmetric states, e.g. $\mathcal{R}^{(2)}$ is a mixture of $|H,H\rangle \pm |V,V\rangle$, $|H,V\rangle + |V,H\rangle$, and either $|H,H\rangle$ or $|V,V\rangle$. We show $\mathcal{R}^{(2)}$ and $\mathcal{R}^{(3)}$ as examples.

$$\mathcal{R}^{(2)} \propto \begin{pmatrix} A_2 & \cdot & \cdot & D_2 \\ & B_2 & B_2 & \cdot \\ & & B_2 & \cdot \\ \text{h.c.} & & & C_2 \end{pmatrix} \tag{5}$$

where the basis is $|H,H\rangle, |H,V\rangle, |V,H\rangle, |V,V\rangle$ and $A_2 \equiv n_{\rm c}^2$, $B_2 = n_{\rm c}(n_{\rm s}+n_{\rm th}+2n_{\rm s}n_{\rm th})$, $C_2 = 3n_{\rm s}^2(1+2n_{\rm th})^2 + n_{\rm s}(1+8n_{\rm th}+12n_{\rm th}^2)+2n_{\rm th}^2$, and $D_2 = n_{\rm c}\sqrt{n_{\rm s}(n_{\rm s}+1)}(1+2n_{\rm th})$. The symbol "$\cdot$" indicates a zero entry, while "h.c." indicates the lower-triangular portion of the (hermitian) matrix. In the limit of zero noise $n_{\rm th} \to 0$, and small flux $n_{\rm s} = n_{\rm c}^2 \to 0$, $\mathcal{R}^{(2)}$ describes a Bell state $\propto |HH\rangle + |VV\rangle$.

Similarly,

$$\mathcal{R}^{(3)} \propto \begin{pmatrix} A_3 & \cdot & \cdot & E_3 & \cdot & E_3 & E_3 & \cdot \\ & B_3 & B_3 & \cdot & B_3 & \cdot & \cdot & F_3 \\ & & B_3 & \cdot & B_3 & \cdot & \cdot & F_3 \\ & & & C_3 & \cdot & C_3 & C_3 & \cdot \\ & & & & B_3 & \cdot & \cdot & F_3 \\ & & \text{h.c.} & & & C_3 & C_3 & \cdot \\ & & & & & & C_3 & \cdot \\ & & & & & & & D_3 \end{pmatrix} \tag{6}$$

where $A_3 = n_\mathrm{c}^3, B_3 = n_\mathrm{c}^2(n_\mathrm{s} + n_\mathrm{th} + 2n_\mathrm{s}n_\mathrm{th}), C_3 = n_\mathrm{c}[3n_\mathrm{s}^2(1 + 2n_\mathrm{th}) + n_\mathrm{s}(1 + 8n_\mathrm{th} + 12n_\mathrm{th}^2) + 2n_\mathrm{th}^2], D_3 = 3(n_\mathrm{s} + n_\mathrm{th} + 2n_\mathrm{s}n_\mathrm{th})[2n_\mathrm{th}^2 + n_\mathrm{s}(1 + 2n_\mathrm{th})(3 + 10n_\mathrm{th}) + 5(n_\mathrm{s} + 2n_\mathrm{s}n_\mathrm{th})^2], E_3 = n_\mathrm{c}^2\sqrt{n_\mathrm{s}(1 + n_\mathrm{s})}(1 + 2n_\mathrm{th}), F_3 = 3n_\mathrm{c}\sqrt{n_\mathrm{s}(1 + n_\mathrm{s})}(1 + 2n_\mathrm{th})(n_\mathrm{s} + n_\mathrm{th} + 2n_\mathrm{s}n_\mathrm{th})$. In the same limit, $\mathcal{R}^{(3)}$ describes a state $\propto |HHH\rangle + |HVV\rangle + |VHV\rangle + |VVH\rangle$ with maximal 3-tangle [33].

Multi-partite entanglement - To explore the entanglement properties with larger photon numbers, we study the reduced two-photon density matrix, obtained by tracing over the last $N - 2$ photons

$$\mathcal{R}^{(2,N)} \equiv \mathrm{Tr}_{3\ldots N}[\mathcal{R}^{(N)}]. \tag{7}$$

By permutation symmetry, an entangled $\mathcal{R}^{(2,N)}$ implies that no partition of $\mathcal{R}^{(N)}$ is separable, i.e., N-partite entanglement. As shown in the Appendix, $\mathcal{R}^{(2,N)}$ can be computed in $O(N^3)$ time using phase-space methods.

Reduction to pure states - We can simplify calculation of $\mathcal{R}^{(N)}$ by considering the effect of polarization-independent losses. If $a_{i,\pi} \overset{\text{loss}}{\to} a_{i,\pi}\sqrt{\eta} + a_{i,\pi}^{(\text{res})}\sqrt{1-\eta}$ where η is the transmission and $a_{i,\pi}^{(\text{res})}$ describe reservoir modes (assumed vacuum), then $R^{(N)} \overset{\text{loss}}{\to} \eta^N R^{(N)}$ and $\mathcal{R}^{(N)}$ is unchanged. At the same time, $n_\mathrm{c} \overset{\text{loss}}{\to} \eta n_\mathrm{c}$, and $\mathrm{var}(q) \overset{\text{loss}}{\to} \eta\,\mathrm{var}(q) + (1-\eta)/4$, where $q \in \{x, p\}$, from which we find that any mixed squeezed state ρ, with n_c, n_s, n_th, can be produced from a pure state ρ' with $n'_\mathrm{c} = n_\mathrm{c}/\eta$, $n'_\mathrm{s} = (n_\mathrm{s} + 2n_\mathrm{s}n_\mathrm{th} + n_\mathrm{th})/\eta$ and $n'_\mathrm{th} = 0$ for $\eta = (n_\mathrm{s} + 2n_\mathrm{s}n_\mathrm{th} - n_\mathrm{th}^2)/(n_\mathrm{s} + 2n_\mathrm{s}n_\mathrm{th} + n_\mathrm{th})$.

Likely outcomes are entangled - For pure states, i.e., $n_\mathrm{th} = 0$, we compute the observable concurrence $\mathcal{C}$, i.e., the concurrence computed on $\mathcal{R}^{(2,N)}$, shown in Figure 3. In all cases, Wineland-criterion squeezing $n_\mathrm{s} > 0$ gives nonzero concurrence. For example, with $n_\mathrm{c} = 100$, $n_\mathrm{s} = 0.3$, and $N = 100$,

$$\mathcal{R}^{(2,100)} \approx \begin{pmatrix} 0.9440 & \cdot & \cdot & 0.0293 \\ \cdot & 0.0270 & 0.0270 & \cdot \\ \cdot & 0.0270 & 0.0270 & \cdot \\ 0.0293 & \cdot & \cdot & 0.0021 \end{pmatrix}. \tag{8}$$

The concurrence is $\mathcal{C} \approx 0.00468$, which is 4.7% of that allowed by monogamy [34], i.e., $\mathcal{C}_\mathrm{max} = 1/\sqrt{N-1} \approx 0.10$. $\mathcal{R}^{(2,N)}$ does not depend strongly on N, and the likely outcomes $n_\mathrm{c} - \sqrt{n_\mathrm{c}} \leq N \leq n_\mathrm{c} + \sqrt{n_\mathrm{c}}$ have similar $\mathcal{C}/\mathcal{C}_\mathrm{max}$. In this sense, post-selection is not necessary to prepare or observe the entanglement. For these likely states, $\mathcal{C}$ peaks for $n_\mathrm{s} \approx 0.3$, or ≈ 4.5 dB of squeezing. We conjecture that 3-tangle and higher-order entanglements compete with $\mathcal{C}$ as n_s grows.

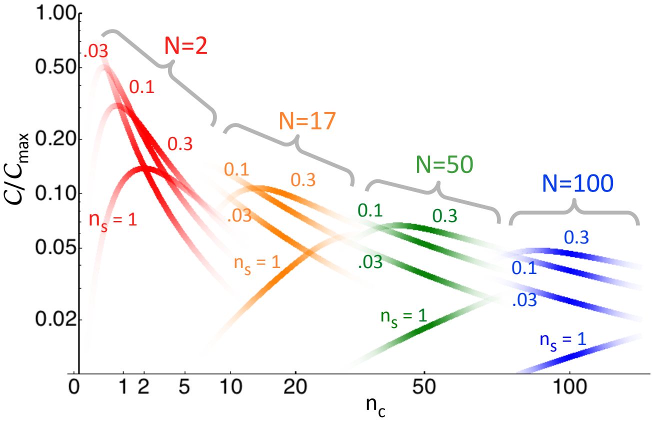

FIG. 3. (color online) Scaled concurrence $\mathcal{C}/\mathcal{C}_\mathrm{max}$ as a function of N, n_c, and n_s for pure states, i.e., $n_\mathrm{th} = 0$. Here $\mathcal{C}_\mathrm{max} = 1/\sqrt{N-1}$ is the largest concurrence allowed by entanglement monogamy [34], shown for $N = 2$ (red), $N = 17$ (orange), $N = 50$ (green) and $N = 100$ (blue). Labels indicate n_s values, and line strength indicates the likelihood of observing N photons from the coherent state with n_c average photons, calculated as $P_N(n_\mathrm{c})/P_N(N)$, where $P_N(\lambda)$ is the Poisson distribution.

Prospects for observation - Due to its structure, $\mathcal{R}^{(2,N)}$ is negative under partial transpose if $\Delta \equiv |\mathcal{R}_{1,4}^{(2,N)}| - \mathcal{R}_{2,3}^{(2,N)} > 0$, e.g. if $0.0293 > 0.0270$ in $\mathcal{R}^{(2,100)}$ above. For $n_\mathrm{c} = N$ in the range 2 to 100 and n_s chosen to maximize $\mathcal{C}$, we find $\Delta = 0.23/N$ to within 10%. Although reconstruction of general N-particle states requires resources exponential in N, here the method of preparation ensures permutation invariance (PI), allowing use of PI reconstruction methods to avoid exponential costs [35] . In particular, we can find $R^{(2,N)}$ by averaging all pairs of detected photons, i.e., $N(N-1)$ pairs per shot, giving single-shot statistical errors of $\delta\Delta \sim 1/N$. We then need $O(N^0)$ shots to establish $\Delta > 0$ with unit signal-to-noise. In light of the N^0 scaling of both production and characterization of entanglement, N may be limited by the performance of available detectors. In this regard, electron-multiplied charge-coupled device (EMCCD) sensors are promising. They can have $M = 2^{20} > 10^6$ pixels, 90% quantum efficiency, negligible dark-count rates, single-photon sensitivity, and some degree of photon-number discrimination for < 5 photons at a given pixel [36]. Evaluating the effect of imperfect detection on $\mathcal{R}$ is beyond the scope of this work, but we note that for $N^2 < M$, fewer than one pixel on average receives multiple photons, so that entangled states with $N \sim 1000$ should be detectable even without photon-number resolution.

Conclusion - In analogy with "extreme spin squeezing," in which squeezing of collective spin variables implies highly multi-partite entanglement of the constituent particles, we have quantified the photonic entanglement of a practical polarization-squeezed state. We find that Wineland-criterion squeezing implies entanglement of a macroscopic fraction of the total photons present. It also implies N-partite entanglement in the observable N-photon density matrix as computed by Glauber photodetection theory. This entanglement is considerable even for modest squeezing and highly robust against losses, making ~1000-partite entanglement observable with existing methods.

This work was inspired by [21]. We thank P. Hyllus, J. K. Korbicz and G. Messin for helpful discussions. Supported by the Spanish MINECO project MAGO (Ref. FIS2011-23520) and by the European Research Council project AQUMET.

Appendix I: Large-J Sørensen-Mølmer-Hyllus theory - For a given system size J, minimization of $\langle J_H \rangle \equiv \langle J_x^2 - \mu J_z \rangle$ over spin states gives a state, parametrized by μ, with scaled noise $\mathcal{V} \equiv \langle J_x^2 \rangle / J$ and polarization $\mathcal{Z} \equiv \langle J_z \rangle / J$. These parametrized values describe a curve at the boundary between possible and impossible $(\mathcal{V}, \mathcal{Z})$ values for that J. k is the minimum J for which a given $(\mathcal{V}, \mathcal{Z})$ is possible.

For highly polarized states, we can approximate the spin raising operator $J_+ |J, m\rangle = \sqrt{J(J+1) - m(m+1)}\, |J, m+1\rangle$ as $J_+ \approx b\sqrt{2J+1}$ where b is the annihilation operator for the defect $\delta_Z \equiv J - J_z$, i.e., if $|\delta_Z\rangle = |J, J - \delta_Z\rangle$, then $b|\delta_Z\rangle = \sqrt{\delta_Z}\, |\delta_Z - 1\rangle$. This geometrical change neglects terms of order $\sqrt{\mathcal{D}}$ where $\mathcal{D} \equiv \delta_Z / J$ [37].

Using $J_x^2 = (J_+ + J_-)^2/4$, $J_- \equiv J_+^\dagger$, we find $J_H \approx (2J+1)(b+b^\dagger)^2/4 + \mu b^\dagger b$ is quadratic in $b, b^\dagger$ and thus reducible to $J_H = A c^\dagger c + B$ by a Bogoliubov transformation $b \to c\cosh r + c^\dagger \sinh r$. The minimum state $|\phi\rangle$ is squeezed vacuum satisfying $c|\phi\rangle = 0$, and as such has $2\langle J_x^2 \rangle / J = 1 + 2\delta_Z - 2\sqrt{\delta_Z(1+\delta_Z)}$ [38]. Allowed states thus satisfy $2\mathcal{V} \geq 1 + 2J\mathcal{D} - 2\sqrt{J\mathcal{D}(1+J\mathcal{D})}$ or $k \approx J(1-2\mathcal{V})^2/(8\mathcal{V}\delta_Z)$ for $\mathcal{V} < 1/2$.

With the squeezed thermal state, $S_0, S_x, \mathrm{var}(S_z)$ play the role of $J, J_z, \mathrm{var}(J_x)$, respectively and we have $\delta_Z = S_0 - S_x = (n_\mathrm{s} + n_\mathrm{th} + 2n_\mathrm{s} n_\mathrm{th})/2$ and $\mathcal{V} = \mathrm{var}(S_z)/S_0 = \frac{1}{2} n_\mathrm{c}(1 + 2n_\mathrm{s} - 2\sqrt{n_\mathrm{s}(n_\mathrm{s}+1)})(1 + 2n_\mathrm{th})/(n_\mathrm{c} + n_\mathrm{s} + n_\mathrm{th} + 2n_\mathrm{s} n_\mathrm{th})$. In the macroscopic limit $n_\mathrm{c} \to \infty$, $k \propto \langle S_0 \rangle$ (see Figure 2).

Appendix II: correlation functions - From [39] pp. 92-94, we can evaluate normally-ordered correlations in terms of the Wigner distribution W as

$$E_{m,n} \equiv \langle (a^\dagger)^m a^n \rangle = \int dx\, dp\, W(x,p) O_{m,n}(x,p), \quad (9)$$

$$O_{m,n} \equiv \lim_{\beta,\beta^* \to 0} \left[\partial_\beta + \frac{\beta^*}{2}\right]^m \left[\partial_{\beta^*} + \frac{\beta}{2}\right]^n \frac{e^{i\beta^* \alpha + i\beta\alpha^*}}{i^{m+n}}, \quad (10)$$

$\alpha \equiv x + ip$. This evaluates to the efficiently computed $O_{m,n>m} = \alpha^{n-m} \sum_{a=0}^m |\alpha|^{2a} \Upsilon_{m,n,a}$, $O_{m,n<m} = O^*_{n,m}$ where

$$\Upsilon_{m,n,a} \equiv (-2)^{a-m} n! m! / [a!(a+n-m)!(m-a)!]. \quad (11)$$

Using the Wigner distribution of a squeezed thermal state

$$W(x,p) = \frac{2}{\pi T^2} \exp[-\frac{2x^2}{T^2 A^2}] \exp[-\frac{2p^2 A^2}{T^2}], \quad (12)$$

and recalling $A = \sqrt{1 + n_\mathrm{s}} + \sqrt{n_\mathrm{s}}$, $T^2 = 1 + 2n_\mathrm{th}$, we find $E_{m,n} = \sum_{a=0}^m \Upsilon_{m,n,a} I_{m,n,a}$ where

$$I_{m,n,a} \equiv \int dx dp\, W(x,p)(x+ip)^{n-m}(x^2+p^2)^a. \quad (13)$$

Defining $t \equiv (n-m)/2$, these evaluate to

$$I_{m,n,a} = \sum_{u=0}^{t} \sum_{b=0}^{a} \begin{pmatrix} 2t \\ 2u \end{pmatrix} \begin{pmatrix} a \\ b \end{pmatrix} \frac{(-1)^{t-u}}{4^{t+a}} A^{2(2u+2b-t-a)} T^{2(t+a)} \times (2(t-u+a-b)-1)!!(2(u+b)-1)!! \quad (14)$$

for $n - m$ even, and zero otherwise.

Appendix III: Reduced density matrix - We calculate

$$R^{(2,N)}_{|p_1,p_2\rangle,\langle p_1',p_2'|} = \sum_{\{p_3 \ldots p_N\} \in \{H,V\}} \langle a^\dagger_{p_1} a^\dagger_{p_2} a^\dagger_{p_3} \ldots a_{p_3} a_{p_2'} a_{p_1'} \rangle \quad (15)$$

with respect to the state in Eq. (1). Defining r, s as the number of V polarizations in $\{p_1, p_2\}$ and $\{p_1', p_2'\}$, respectively, we find

$$R^{(2,N)}_{|p_1,p_2\rangle,\langle p_1',p_2'|} = \sum_{m=0}^{N-2} \begin{pmatrix} N-2 \\ m \end{pmatrix} (\alpha_H^*)^{N-m-r} \alpha_H^{N-m-s} \times E_{r+m,s+m}. \quad (16)$$

Calculations in Mathematica are available as an ancillary file, "ExtremeSpinSqueezingForPhotons.nb"

---

[*] morgan.mitchell@icfo.es

[†] federica.beduini@icfo.es

[1] H. Häffner, W. Hänsel, C. F. Roos, *et al.*, Nature **438**, 643 (2005).

[2] C. Negrevergne, T. S. Mahesh, C. A. Ryan, M. Ditty, F. Cyr-Racine, W. Power, N. Boulant, T. Havel, D. G. Cory, and R. Laflamme, Phys. Rev. Lett. **96**, 170501 (2006).

[3] P. Neumann, N. Mizuochi, F. Rempp, *et al.*, Science **320**, 1326 (2008).

[4] M. W. Mitchell, J. S. Lundeen, and A. M. Steinberg, Nature **429**, 161 (2004).

[5] C. Y. Lu, X. Q. Zhou, O. Gühne, *et al.*, Nature Physics **3**, 91 (2007).

[6] W. Wieczorek, R. Krischek, N. Kiesel, *et al.*, Physical Review Letters **103**, 020504 (2009).

[7] T. Monz, P. Schindler, J. T. Barreiro, *et al.*, Physical Review Letters **106**, 130506 (2011).

[8] A. Sørensen, L.-M. Duan, J. I. Cirac, and P. Zoller, Nature **409**, 63 (2001).

[9] G. Vitagliano, P. Hyllus, I. n. L. Egusquiza, and G. Tóth, Phys. Rev. Lett. **107**, 240502 (2011).

[10] A. S. Sørensen and K. Mølmer, Phys. Rev. Lett. **86**, 4431 (2001).

[11] J. K. Korbicz, J. I. Cirac, and M. Lewenstein, Physical Review Letters **95**, 120502 (2005).

[12] J. K. Korbicz, O. Gühne, M. Lewenstein, H. Häffner, C. F. Roos, and R. Blatt, Phys. Rev. A **74**, 052319 (2006).

[13] O. Gühne and G. Tóth, Physics Reports **474**, 1 (2009).

[14] C. Gross, T. Zibold, E. Nicklas, J. Esteve, and M. Oberthaler, Nature **464**, 1165 (2010).

[15] J. Appel, P. J. Windpassinger, D. Oblak, U. Hoff, N. Kjaergaard, and E. S. Polzik, Proc. Nat. Acad. Sci. **106**, 10960 (2009).

[16] I. D. Leroux, M. H. Schleier-Smith, and V. Vuletic, Phys. Rev. Lett. **104**, 073602 (2010).

[17] M. Koschorreck, M. Napolitano, B. Dubost, N. Behbood, R. Sewell, and M. W. Mitchell (2010).

[18] Z. Chen, J. G. Bohnet, S. R. Sankar, J. Dai, and J. K. Thompson, Phys. Rev. Lett. **106**, 133601 (2011).

[19] R. J. Sewell, M. Koschorreck, M. Napolitano, B. Dubost, N. Behbood, and M. W. Mitchell, Phys. Rev. Lett. **109**, 253605 (2012).

[20] R. J. Glauber, Phys. Rev. **130**, 2529 (1963).

[21] K. Mølmer, Phys. Rev. A **55**, 3195 (1997).

[22] N. Korolkova, G. Leuchs, R. Loudon, T. C. Ralph, and C. Silberhorn, Phys. Rev. A **65**, 052306 (2002).

[23] W. P. Bowen, N. Treps, R. Schnabel, and P. K. Lam, Phys. Rev. Lett. **89**, 253601 (2002).

[24] A. Predojevic, Z. Zhai, J. M. Caballero, and M. W. Mitchell, Phys. Rev. A **78** (2008), 10.1103/PhysRevA.78.063820.

[25] J. Ries, B. Brezger, and A. I. Lvovsky, Phys. Rev. A **68**, 025801 (2003).

[26] R. Schnabel, W. P. Bowen, N. Treps, T. C. Ralph, H.-A. Bachor, and P. K. Lam, Phys. Rev. A **67**, 012316 (2003).

[27] D. J. Wineland, J. J. Bollinger, W. M. Itano, and D. J. Heinzen, Phys. Rev. A **50**, 67 (1994).

[28] P. Hyllus, L. Pezzé, A. Smerzi, and G. Tóth, Phys. Rev. A **86**, 012337 (2012).

[29] P. Erdös and A. Rényi, Publ. Math. Inst. Hung. Acad. Sci., Ser. A **5**, 17 (1960).

[30] A. Acin, J. I. Cirac, and M. Lewenstein, Nat Phys **3**, 256 (2007).

[31] M. Cuquet and J. Calsamiglia, Phys. Rev. Lett. **103**, 240503 (2009).

[32] D. F. V. James, P. G. Kwiat, W. J. Munro, and A. G. White, Physical Review A **64**, 52312 (2001).

[33] V. Coffman, J. Kundu, and W. K. Wootters, Phys. Rev. A **61**, 052306 (2000).

[34] W. K. Wootters, Phys. Rev. Lett. **80**, 2245 (1998).

[35] G. Tóth, W. Wieczorek, D. Gross, R. Krischek, C. Schwemmer, and H. Weinfurter, Phys. Rev. Lett. **105**, 250403 (2010).

[36] C. Mackay, T. D. Staley, D. King, F. Suess, and K. Weller, in *Proc. SPIE 7742, High Energy, Optical, and Infrared Detectors for Astronomy IV* (2010) pp. 774202–774202–11.

[37] F. T. Arecchi, E. Courtens, R. Gilmore, and H. Thomas, Phys. Rev. A **6**, 2211 (1972).

[38] A numerical calculation, using J_H truncated to the subspace $J - d \le m \le J$ and increasing d until convergence, agrees with this approximation with an error in $\langle J_x^2 \rangle$ of at most $5\sqrt{\delta_Z}/(2J)$ for $0 \le \delta_Z \le 2$, corresponding to up to 10 dB of squeezing.

[39] M. Scully and M. Zubairy, *Quantum Optics* (Cambridge University Press, 1997).